

# Experimental Investigation of the CO<sub>2</sub> Huff and Puff Effect in Low-Permeability Sandstones with NMR

Jinsheng Zhao,\* Pengfei Wang, Haien Yang, Fan Tang, Yingjun Ju, and Yuqin Jia

Cite This: *ACS Omega* 2021, 6, 15601–15607

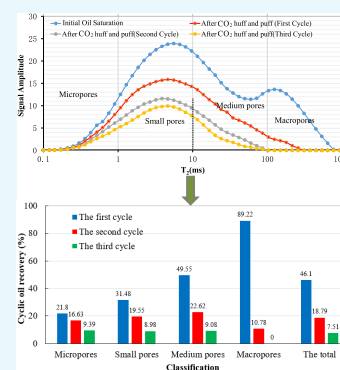
Read Online

ACCESS |

Metrics &amp; More

Article Recommendations

**ABSTRACT:** For low-permeability sandstone reservoirs, CO<sub>2</sub> huff and puff is an effective method for increasing oil recovery. Commonly, sandstone formations with low permeability have diverse pore and throat sizes and a complex pore-throat structure, which essentially affects the flow characteristics of CO<sub>2</sub> and oil in the formation and further the CO<sub>2</sub> huff and puff performance. It is necessary to understand the recovery degree of various microscale pore sizes under different operational parameters during CO<sub>2</sub> huff and puff in tight sandstones. In this work, several experiments of cyclic CO<sub>2</sub> injection are conducted with sandstone core samples with low permeability. Before and after the injection, the  $T_2$  spectra of the sandstone cores are compared using the NMR technique. We then discuss the micro residual oil distribution and recovery degree in different pores, such as micropores (<1 ms), small pores (1–10 ms), medium pores (10–100 ms), and macropores (>100 ms). It is found that the recovery degree in the different pores increases as the pore size increases. Oil can be recovered more easily from macropores and medium pores during the cyclic CO<sub>2</sub> injection. The oil contained in micropores is relatively difficult to extract considering a high capillary force under immiscible conditions. It is found that the total recovery degree increases with the increase in soaking time. However, such a recovery degree increment in small pores is not as large as that achieved in medium and large pores. With the CO<sub>2</sub> injection volume increase, the total recovery degree increases. When the CO<sub>2</sub> injection volume is less than 1.5 PV, it is challenging to extract the oil from micropores and small pores. As the cycle number increases, the cyclic oil recovery decreases, and most of the oil is produced in the first cycle. This suggests that under the experimental conditions of this study, the cycle number of CO<sub>2</sub> huff and puff shall not be more than 3. This work is important to further understand the CO<sub>2</sub> huff and puff process for improving oil recovery in sandstone reservoirs with low permeability.



## 1. INTRODUCTION

To decrease the CO<sub>2</sub> emissions and greenhouse effect, numerous efforts have been made on carbon capture, utilization, and storage (CCUS).<sup>1–4</sup> On the other hand, to replenish formation energy, low-permeability reservoirs are usually developed by water injection or gas injection.<sup>5,6</sup> CO<sub>2</sub> injection can increase oil production by oil expansion, reducing oil–water interfacial tension and oil viscosity, and light hydrocarbon extraction from oil.<sup>7,8</sup> Therefore, for low-permeability reservoirs, CO<sub>2</sub> injection has been recognized as an effective method for enhancing oil recovery.<sup>9,10</sup> The methods of CO<sub>2</sub> injection for enhancing oil recovery include CO<sub>2</sub> flooding, CO<sub>2</sub> huff and puff, and CO<sub>2</sub>–water alternate injection.<sup>2</sup> As for a single well, CO<sub>2</sub> huff and puff is more workable and practical taking into account the low cost with a high return feature.<sup>7,11</sup> Pore and throat sizes of tight sandstone formations are typically on the micro- and nanoscale combined with complex pore-throat structure, which significantly impacts the production degree in different pores and throats during CO<sub>2</sub> huff and puff. Hence, the study of the remaining oil distribution in different pores is helpful to understand the mechanisms of CO<sub>2</sub> huff and puff in sandstone reservoirs with low permeability.

Numerous works have been done to study the injection parameters that affect the performance of cyclic CO<sub>2</sub> injection,<sup>12–15</sup> including soaking time, injection volume, injection mode, injection pressure, etc. Kong et al. probed and analyzed the performance of water flooding and CO<sub>2</sub> huff and puff in a tight oil reservoir. The results showed that the length of the gas injection stage and production stage can impose a greater influence on the cyclic CO<sub>2</sub> injection performance compared with the soaking time in each cycle.<sup>16</sup> Firouz and Torabi experimentally investigated the influence of the shut-in time on the effect of the CO<sub>2</sub> huff and puff. A long soaking time can effectively increase the recovery degree of the first cycle; however, it cannot noticeably increase the ultimate oil recovery.<sup>17</sup> Wang et al. optimized the injection parameters and found that the optimum injection time and soaking time

Received: December 23, 2020

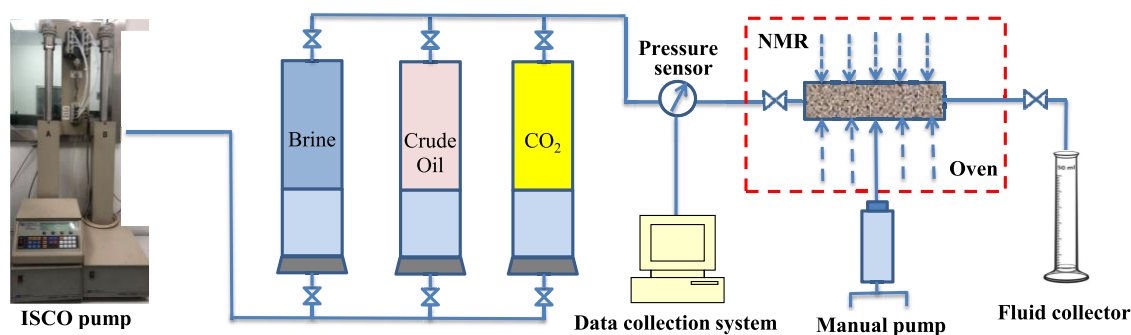
Accepted: May 25, 2021

Published: June 9, 2021



Table 1. Cores and Operational Parameters of CO<sub>2</sub> Huff and Puff

core no.	length (cm)	radius (cm)	permeability ( $10^{-3} \mu\text{m}^2$ )	porosity (%)	injection pressure (MPa)	injection volume (PV)	soaking time (h)	number of cycles
1	4.15	2.50	0.47	9.36	7.2	0.15	5	1
2	3.91	2.50	0.52	9.89	7.4	0.15	10	1
3	3.94	2.50	0.67	10.03	7.3	0.15	15	1
4	4.39	2.50	5.85	10.24	6.2	0.1	10	1
5	4.32	2.50	5.70	12.05	7.5	0.15	10	1
6	4.02	2.50	5.93	10.89	8.8	0.2	10	1
7	3.52	2.50	3.0	9.53	9.0	0.2	15	3

Figure 1. Flow chart of the cyclic CO<sub>2</sub> injection experiment.

are 1 year and 30 days, respectively.<sup>18</sup> Zhang et al. found that the main factors affecting the CO<sub>2</sub> huff and puff effect include CO<sub>2</sub> injection volume, permeability, and stress sensitivity.<sup>19</sup> Song and Yang evaluated field-scale CO<sub>2</sub> huff and puff performance in the Bakken reservoir. This study suggested that a high injection pressure or a low production pressure usually results in better recovery performance, while the maximum recovery degree can be achieved under the condition of soaking time of 15 days.<sup>20</sup>

Nuclear magnetic resonance (NMR) technology is usually utilized to test the distribution of fluid containing hydrogen in a porous medium. When the fluid containing hydrogen is placed in a porous medium, the hydrogen nucleus in the fluid makes a movement of transverse relaxation.<sup>21,22</sup> The larger the pore size, the longer the corresponding transverse relaxation time ( $T_2$ ).<sup>23,24</sup> Therefore, the  $T_2$  spectrum distribution also indicates the pore size distribution, and the NMR technique can be used to determine the pore size distribution.<sup>25–27</sup> Several researchers have conducted analyses to better understand the performance of CO<sub>2</sub> huff and puff on the microscale through NMR techniques.<sup>28–30</sup> Wei et al. discussed the oil distribution in the matrix and fractures of cores with a low-field NMR measurement. The results demonstrated that the produced oil was initially from large pores with a  $T_2$  value from 3.0 to 100 ms.<sup>28</sup> Ma and Bai applied the NMR technique to analyze the residual oil distribution in different pores. It was found that the produced oil is mainly from large and medium pores for the first cycle. In the succeeding cycles, the remaining oil is generally produced from the smaller pores and micropores.<sup>29–32</sup> For CO<sub>2</sub> huff and puff in low-permeability sandstone reservoirs, although previous studies have investigated the oil recovery degree from different pore sizes, the change of the pore size range where the oil is produced at different operation parameters such as injection pressure, injection volume, and soaking time is not yet systematically investigated, which, nevertheless, is crucial to understand the

process of cyclic CO<sub>2</sub> injection for increasing oil recovery in sandstone formations with low permeability.

In this study, the NMR technique is employed to investigate the CO<sub>2</sub> huff and puff effect at different operation parameters such as soaking time, injection volume, and cycle numbers. According to comparison of the  $T_2$  spectrum before and after CO<sub>2</sub> huff and puff, the residual oil saturation and recovery factor in different pores are discussed. This paper aims to investigate the process of CO<sub>2</sub> huff and puff as an efficient method to improve oil recovery in tight formations.

## 2. EXPERIMENT AND METHODS

**2.1. Materials.** The seven sandstone cores used for the study are from the Chang 8 reservoir of the Heshui oilfield in China. Table 1 gives the core sizes, rock properties, and experimental parameters. The experimental oil is made up of degassed crude oil and kerosene in a volume ratio of 1:3. The viscosity and density of the oil are 2.16 mPa·s and 0.8 g/cm<sup>3</sup> at 323.15 K, respectively. The water used to saturate the cores has MnCl<sub>2</sub> with a mass concentration of 25 000 mg/L; the hydrogen content is eliminated in the liquid. The purity of the CO<sub>2</sub> used in the experiment is 99.99 mol %, and the minimum miscibility pressure (MMP) at 323.15 K is measured to be 17.5 MPa.

**2.2. Experimental Setup.** Figure 1 presents the flow chart of the CO<sub>2</sub> huff and puff experiment. NMR equipment (Geo spec2/53, Oxford, England) is applied to measure the  $T_2$  spectrum of the sandstone cores. An ISCO pump (A100DX, Teledyne ISCO) is used to inject fluid into the cores with an accuracy of 0.5% of the set flow rate. A manual pump (Hongbo Co. Ltd., China) is used to maintain the confinement pressure of the cores. The measured data of flow rate and pressure are recorded by a data collection system.

**2.3. Experimental Steps.** The cyclic CO<sub>2</sub> injection experiment in the sandstone cores is first conducted. The recovery factors and residual oil saturations for different pore sizes are compared by analyzing the  $T_2$  spectrum before and

after CO<sub>2</sub> huff and puff. The following experimental steps are taken:

- (1) The seven cores are completely cleaned using benzene to remove the oil contained in the cores.
- (2) The cleaned cores are dried at 363.15 K for 12 h to remove the residual benzene and moisture.
- (3) The dried cores are measured for permeability and then saturated with MnCl<sub>2</sub> aqueous solution.
- (4) The cores saturated with MnCl<sub>2</sub> solution are saturated with oil by displacing water.
- (5) NMR equipment is then applied to measure the T<sub>2</sub> spectrum of the cores saturated with oil. Through analyzing the measured T<sub>2</sub> spectrum, the initial oil distribution in different pore sizes can be obtained.
- (6) Then, the CO<sub>2</sub> huff and puff experiment is conducted. First, the core holder outlet is closed, and then the core is injected with CO<sub>2</sub> at a rate of 0.1 mL/min until the injected volume reaches the volume shown in Table 1. Then, the core holder inlet is closed, and the core is aged for a soaking time also shown in Table 1. After that, the core holder inlet is opened, and the oil is produced. During the cyclic CO<sub>2</sub> injection of every core, injection pressure and cycle number are set as given in Table 1. The experimental temperature is kept constant at 50 °C.
- (7) Once the CO<sub>2</sub> huff and puff experiment is completed, the cores are scanned and the T<sub>2</sub> spectrum is measured again. This can be used to determine the remaining oil saturation in the cores after the CO<sub>2</sub> huff and puff process. Based on the T<sub>2</sub> spectrum before and after CO<sub>2</sub> huff and puff, the recovery degree in different pore sizes can be determined by the equation given below

$$R = \frac{S_0 - S}{S_0} \quad (1)$$

where  $R$  represents the recovery factor after the cyclic CO<sub>2</sub> injection;  $S_0$  means the area covered by the original T<sub>2</sub> spectrum and X-axis before the CO<sub>2</sub> huff and puff; and  $S$  is the area covered by the T<sub>2</sub> spectrum and X-axis after CO<sub>2</sub> huff and puff.

- (8) Comparing and analyzing the T<sub>2</sub> spectra before and after the cyclic CO<sub>2</sub> injection for the oil in the cores, the remaining oil saturation in various pore sizes can be obtained and is discussed.

### 3. RESULTS AND DISCUSSION

**3.1. Influence of Soaking Time on the Oil Recovery Factor.** To determine the true pore size, a core sample from the same area is selected for the mercury injection test and NMR test. The test results are shown in Figures 2 and 3. The corresponding values of the peak values of the two curves are 0.4 μm and 58.73 ms. The division of the two values determines that the conversion coefficient of the pore radius and T<sub>2</sub> value is 0.007.

Figures 4–6 show the T<sub>2</sub> spectrum distributions of cores #1, #2, and #3 before and after the cyclic CO<sub>2</sub> injection with

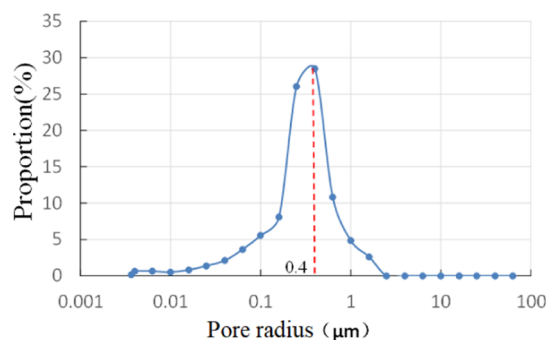


**Figure 2.** Pore radius distribution of core #0 tested by the mercury injection experiment.

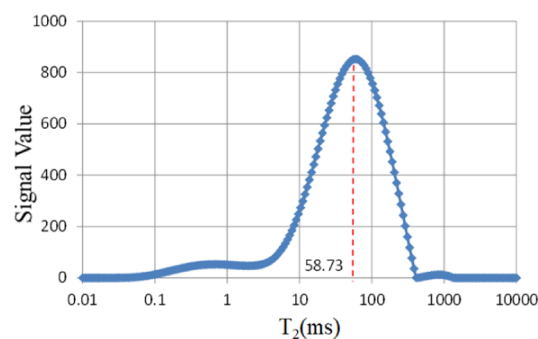


**Figure 3.** T<sub>2</sub> spectrum distribution of core #0 tested by NMR.

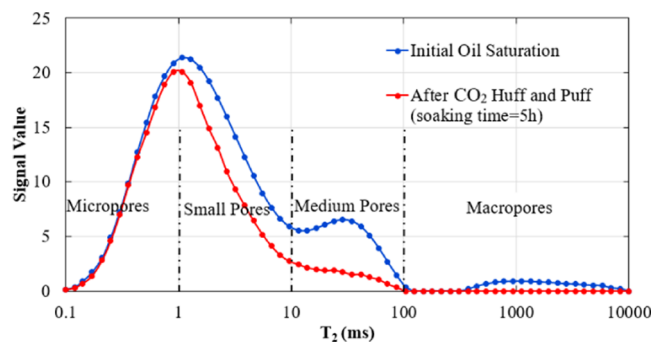


**Figure 4.** T<sub>2</sub> spectrum distribution of core #1, with a 5 h soaking time.

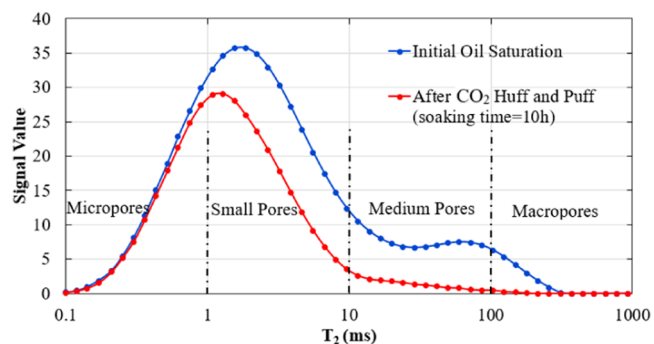


**Figure 5.** T<sub>2</sub> spectrum distribution of core #2, with a 10 h soaking time.

soaking times of 5, 10, and 15 h, respectively. According to the common classification method based on transverse relaxation time, the pores of the cores are classified into four groups, i.e., micropores (diameter smaller than 1 ms), small pores (diameter between 1 and 10 ms), medium pores (diameter

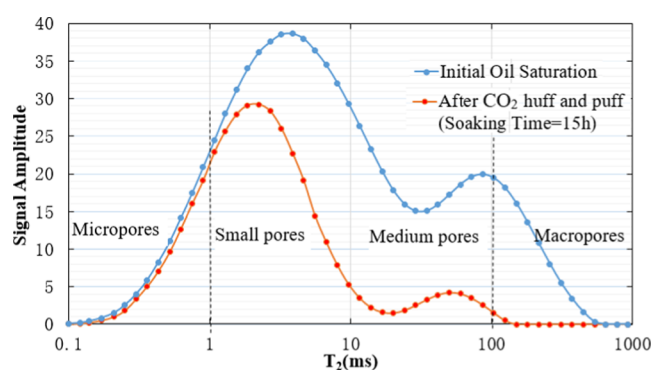


**Figure 6.**  $T_2$  spectrum distribution of core #3, with a 15 h soaking time.

between 10 and 100 ms), and large pores (>100 ms). The true pore size of micropores, small pores, medium pores, and large pores is 0–0.007, 0.007–0.07, 0.07–0.7, and >0.7  $\mu\text{m}$  respectively.

Table 2 gives the oil saturations before and after one  $\text{CO}_2$  huff and puff cycle with different soaking times. The recovery factors of the pore sizes are calculated based on eq 1 and shown in Table 3.

As can be seen in Table 2, the pore sizes of the three cores are mainly in the range of micropores and small pores, and around 60–80% of oil is contained in micropores and small pores. After the first cycle, the percentage of the remaining oil distributed in the micropores and small pores further increases to more than 90%, while the oil in the medium pores and large pores is less than 10%. In other words, the oil in the large and medium pores is easily extracted at the three soaking times compared to that in the micro and small pores. As shown in Figures 4–6, the area covered by the  $T_2$  spectrum curves of the three cores after  $\text{CO}_2$  huff and puff is found to decline to varying degrees compared with the initial  $T_2$  spectrum. However, there is a large difference of the area decreases occurring in the pores with different sizes. It can be observed that a large pore size and a long soaking time will lead to a great decline of areas covered by the  $T_2$  spectrum, i.e., a high recovery degree of the oil. This indicates that both the soaking time and pore size can affect the  $\text{CO}_2$  huff and puff performance. Table 3 further summarizes the calculated recovery factor in the pores with different sizes. One can find that the value of the recovery factor is strongly dependent on the pore size and gradually increases with an increase in the soaking time. However, compared with the soaking time, pore size is definitely the main factor that determines the recovery factor. It can be seen that although the soaking time of core #3 is three times as long as that of core #1, the recovery factor (12.01%) of micropores of core #3 is still less than 1/2 of the

**Table 3. Recovery Factor for Different Pore Sizes after One Cycle**

core no.	soaking time (h)	recovery factor (%)				total
		micropores	small pores	medium pores	macropores	
1	5	4.64	26.37	69.86	100.00	29.23
2	10	7.00	36.24	82.41	95.77	38.30
3	15	12.01	38.57	84.60	97.91	54.84

recovery factor (26.37%) of small pores of core #1, not to mention that the permeability of the former is higher than that of the latter. That is to say, a long soaking time cannot achieve a high increment of the recovery factor of the oil contained in micropores. As for the macropores, the recovery factor of core #1 is larger than those of cores #2 and #3, which is because the pore size of macropores in core #1 is much larger than those of cores #2 and #3.

It should be noted that with a longer soaking time, the total recovery factor of core #3 has a noticeable improvement compared with that of core #2. According to the original  $T_2$  spectrum distributions of the three cores (Figures 4–6), it is found that the left peak value of the  $T_2$  spectrum of core #3 is higher and the span between two peaks is shorter compared with those of cores #1 and #2, which usually means a relatively homogeneous pore size and leads to a better pore-throat connectivity in core #3. Thereby, in addition to a longer soaking time, a better pore-throat connectivity possibly is a reason accounting for the high recovery degree of core #3 after  $\text{CO}_2$  huff and puff.

### 3.2. Influence of Injection Volume on the $\text{CO}_2$ Huff and Puff Effect.

Figures 7–9 show the  $T_2$  spectrum

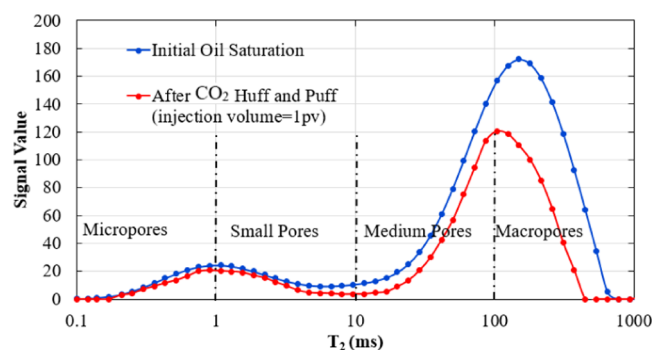


**Figure 7.**  $T_2$  spectrum distribution of core #4 with an injection volume of 1 PV.

distribution of cores #4, #5, and #6 before and after  $\text{CO}_2$  huff and puff with  $\text{CO}_2$  injection volumes of 1.0, 1.5, and 2.0 PV, respectively. With the increase in  $\text{CO}_2$  injection volume,

**Table 2. Oil Saturation after One Cycle with Different Soaking Times**

core no.	conditions	oil saturation (%)			
		micropores (<1 ms)	small pores (1–10 ms)	medium pores (10–100 ms)	macropores (>100 ms)
1	initial oil saturation	30.99	49.18	16.58	3.25
	soaking time of 5 h	41.77	51.17	7.06	0.00
2	initial oil saturation	23.74	57.79	14.96	3.52
	soaking time of 10 h	35.58	59.84	4.33	0.25
3	initial oil saturation	10.28	51.75	26.55	11.42
	soaking time of 15 h	20.04	70.38	9.05	0.53

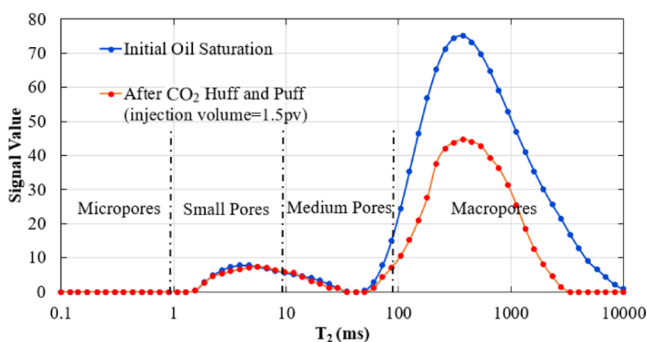


**Figure 8.**  $T_2$  spectrum distribution of core #5 with an injection volume of 1.5 PV.

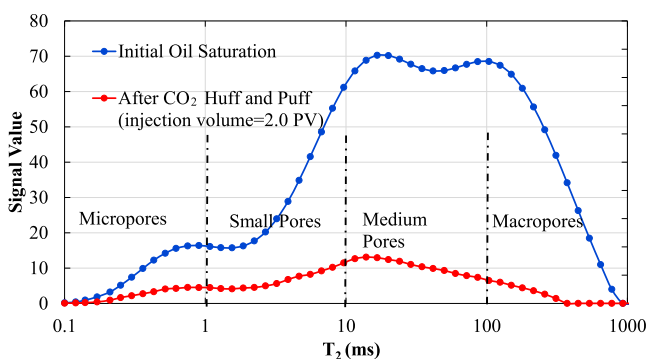


**Figure 9.**  $T_2$  spectrum distribution of core #6 with an injection volume of 2.0 PV.

the decline in the area covered by the  $T_2$  spectrum after CO<sub>2</sub> huff and puff increases, which means that the volume of the produced oil increases. When the injection volumes are 1.0 and 1.5 PV, the produced oil of cores #4 and #5 after CO<sub>2</sub> huff and puff can be observed to be mainly from medium pores and macropores. When the injection volume is increased to 2.0 PV, a large amount of oil is produced from all pores of the core, which includes micropores, small pores, medium pores, and macropores in core #6. Especially, the recovery factor of different pore sizes is in the range of 30.44–85.29% (Table 4).

**Table 4. Recovery Factor for Different Pore Sizes with Different Injected Volumes in One Cycle**

core no.	injection volume (h)	recovery factor (%)				total
		micropores	small pores	medium pores	macropores	
4	5	21.10	28.13	28.33	48.43	39.25
5	10	6.64	36.19	50.76	47.69	47.69
6	15	30.44	45.88	60.88	85.29	62.63

This is likely attributed to the fact that with the increase of the CO<sub>2</sub> injection volume, more CO<sub>2</sub> can intrude into the micropores and small pores, which is conducive to mass transfer between CO<sub>2</sub> and oil and further extract more produced oil from the micropores and small pores due mainly to a lowered interfacial tension and viscosity. In addition, the pressure in the core will increase with the increase in CO<sub>2</sub> injection volume and then cause an increase in the solubility of CO<sub>2</sub> in the crude oil similarly, which will be beneficial to improve the total recovery factor after CO<sub>2</sub> huff and puff. According to the results of the three cores, it is difficult to

produce the oil from micropores and small pores under the conditions of 323.15 K and 7.0 MP, when the CO<sub>2</sub> injection volume is less than 1.5 PV.

**3.3. Influence of Cycle Numbers on the CO<sub>2</sub> Huff and Puff Effect.** Figure 10 shows the  $T_2$  spectrum distribution of

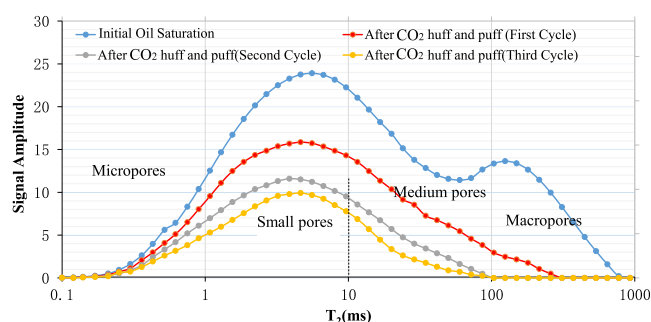


**Figure 10.**  $T_2$  spectrum distribution of core #7 with different cycle numbers.

core #7 before and after CO<sub>2</sub> huff and puff with different cycle numbers. The microscale recovery factors of different pore sizes after every CO<sub>2</sub> huff and puff cycle are calculated and shown in Figure 11. As can be seen in Figure 10, the  $T_2$

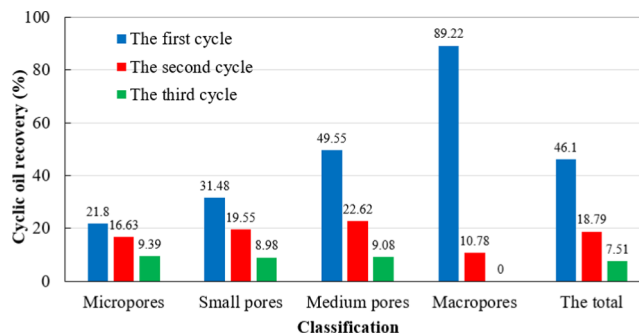


**Figure 11.** Recovery factor of core #7 in various pore sizes with different cycle numbers.

spectrum after CO<sub>2</sub> huff and puff declines to a certain extent after each CO<sub>2</sub> huff and puff cycle. However, the decline becomes gradually smaller. In other words, with the progress of CO<sub>2</sub> huff and puff, oil is continuously produced in the core, and the oil produced by a subsequent cycle of CO<sub>2</sub> huff and puff under the same operating conditions decreases. As shown in Figure 9, for the first cycle, the larger the pore diameter, the more the oil produced, and the corresponding cyclic oil recovery is from 21.8% of micropores to 89.22% of macropores. After the second cycle of CO<sub>2</sub> huff and puff, all of the remaining oil in the macropores has been extracted, and the oil recovery factors of the micropores, small pores, and medium pores gradually increase and reach 16.63, 19.55, and 22.62%, respectively. However, in the third cycle, the cyclic oil recovery in all grades of pores, i.e., micropores, small pores, and medium pores, decreased sharply to less than 10%. It can be inferred that if there are more than three cycles of CO<sub>2</sub> huff and puff, the corresponding cyclic oil recovery rate will be lower. Thereby, under the experimental conditions of this study (see Table 1), the cycle number of CO<sub>2</sub> huff and puff is recommended to be less than 3.

## 4. CONCLUSIONS

The performance of CO<sub>2</sub> huff and puff with different soaking times, injection volumes, and cycle numbers is experimentally investigated using the NMR technique in low-permeability sandstone cores. According to the measured T<sub>2</sub> spectrum before and after cyclic CO<sub>2</sub> injection, the microscale recovery factors for micropores, small pores, medium pores, and macropores are compared. The conclusions drawn are as follows.

- The recovery factor in different pore sizes of the cyclic CO<sub>2</sub> injection is positively correlated with the pore size. Oil in the micropores (<1 ms) is relatively difficult to produce compared with that in macropores and medium pores under immiscible conditions.
- After one CO<sub>2</sub> huff and puff cycle, with the increase in soaking time, the total recovery factor increases to 29.23, 38.30, and 54.84%. The produced oil is observed to be mainly from macropores and medium pores; the increased recovery in micropores is limited depending only on increasing the soaking time.
- With the increase in CO<sub>2</sub> injection volume, the pressure in the core increases, which can be beneficial to improve the total recovery degree after CO<sub>2</sub> huff and puff. Based on the experiments of this work, it is difficult to produce oil from micropores and small pores when the CO<sub>2</sub> injection volume is less than 1.5 PV.
- Comparing the T<sub>2</sub> spectrum distribution before and after a three-cycle CO<sub>2</sub> huff and puff, most of the oil is produced in the first cycle. As for the third cycle of CO<sub>2</sub> huff and puff, the cyclic oil recovery degree in all pores is less than 10%. This suggests that the cycle number of CO<sub>2</sub> huff and puff shall not be more than 3 under the experimental conditions of this work.

## AUTHOR INFORMATION

### Corresponding Author

**Jinsheng Zhao** – Shaanxi Key Laboratory of Advanced Stimulation Technology for Oil & Gas Reservoirs, Xi'an Shiyou University, Xi'an 710065, P. R. China; School of Petroleum Engineering, Xi'an Shiyou University, Xi'an 710065, P. R. China; [orcid.org/0000-0002-8583-683X](https://orcid.org/0000-0002-8583-683X); Phone: +86-29-88382682; Email: [jszhao@xsyu.edu.cn](mailto:jszhao@xsyu.edu.cn); Fax: +86-29-88382682

### Authors

**Pengfei Wang** – Shaanxi Key Laboratory of Advanced Stimulation Technology for Oil & Gas Reservoirs, Xi'an Shiyou University, Xi'an 710065, P. R. China; School of Petroleum Engineering, Xi'an Shiyou University, Xi'an 710065, P. R. China

**Haien Yang** – National Engineering Laboratory of Low-Permeability Oil & Gas Exploration and Development, PetroChina Changqing Oilfield Company, Xi'an 710021, P. R. China; Oil and Gas Technology Research Institute, PetroChina Changqing Oilfield Company, Xi'an 710021, P. R. China

**Fan Tang** – National Engineering Laboratory of Low-Permeability Oil & Gas Exploration and Development, PetroChina Changqing Oilfield Company, Xi'an 710021, P. R. China; Oil and Gas Technology Research Institute, PetroChina Changqing Oilfield Company, Xi'an 710021, P. R. China

**Yingjun Ju** – No. 6 Oil Production Plant, PetroChina Changqing Oilfield Company, Xi'an 710200, P. R. China

**Yuqin Jia** – National Engineering Laboratory of Low-Permeability Oil & Gas Exploration and Development, PetroChina Changqing Oilfield Company, Xi'an 710021, P. R. China; Oil and Gas Technology Research Institute, PetroChina Changqing Oilfield Company, Xi'an 710021, P. R. China

Complete contact information is available at:

<https://pubs.acs.org/10.1021/acsomega.0c04250>

## Notes

The authors declare no competing financial interest.

## ACKNOWLEDGMENTS

This research was supported by the Science and Technology Plan Project of Shaanxi Province (No. 2021JM-411), the Postgraduate Innovation and Practical Ability Cultivation Plan (No. YCS20211003), the National Natural Science Foundation of China (No. 51774236), and the Youth Innovation Team of Shaanxi Universities.

## REFERENCES

- (1) Grimston, M. C.; Karakoussis, V.; Fouquet, R.; Vorst, R. V.; Pearson, P.; Leach, M. The European and global potential of carbon dioxide sequestration in tackling climate change. *Clim. Policy* **2001**, *1*, 155–171.
- (2) Li, B.; Bai, H.; Li, A.; Zhang, L.; Zhang, Q. Experimental investigation on influencing factors of CO<sub>2</sub> huff and puff under fractured low permeability conditions. *Energy Sci. Eng.* **2019**, *7*, 1621–1631.
- (3) Wang, X.; Zeng, F.; Gao, R.; Zhao, X.; Hao, S.; Liang, Q.; Jiang, S. Cleaner coal and greener oil production: An integrated CCUS approach in Yanchang Petroleum Group. *Int. J. Greenhouse Gas Control* **2017**, *62*, 13–22.
- (4) Liu, F.; Ellett, K.; Xiao, Y.; Rupp, J. A. Assessing the feasibility of CO<sub>2</sub> storage in the New Albany Shale (Devonian–Mississippian) with potential enhanced gas recovery using reservoir simulation. *Int. J. Greenhouse Gas Control* **2013**, *17*, 111–126.
- (5) Alhuraishawy, A.; Bai, B.; Wei, M.; Geng, J.; Pu, J. Mineral dissolution and fine migration effect on oil recovery degree by low-salinity water flooding in low-permeability sandstone reservoir. *Fuel* **2018**, *220*, 898–907.
- (6) Das, A.; Nguyen, N.; Farajzadeh, R.; Southwick, J. G.; Vincent-Bonnieu, S.; Khaburi, S.; Kindic, A. Al.; Quo, P. N. Experimental study of injection strategy for Low-Tension-Gas flooding in low permeability, high salinity carbonate reservoirs. *J. Pet. Sci. Eng.* **2020**, *184*, No. 106564.
- (7) Koorosh, A.; Farshid, T. In *Laboratory Experimental Results of Huff-and-Puff CO<sub>2</sub> Flooding in a Fractured Core System*, SPE Annual Technical Conference and Exhibition, Anaheim, California, USA, 2007.
- (8) Huang, T.; Zhou, X.; Yang, H.; Liao, G.; Zeng, F. CO<sub>2</sub> flooding strategy to enhance heavy oil recovery. *Petroleum* **2017**, *3*, 68–78.
- (9) Li, Q.; Li, H.; Xiao, Q. In *Application of CO<sub>2</sub> Miscible Flooding on Gao 89-1 Low Permeability Reservoir*, SPE Asia Pacific Oil and Gas Conference and Exhibition, Jakarta, Indonesia, 2011.
- (10) Li, S.; Zhang, K.; Jia, N.; Liu, L. Evaluation of four CO<sub>2</sub> injection schemes for unlocking oils from low-permeability formations under immiscible conditions. *Fuel* **2018**, *234*, 814–823.
- (11) Haines, H. K.; Monger, T. G. In *A Laboratory Study of Natural Gas Huff "N" Puff*, CIM/SPE International Technical Meeting, Calgary, Alberta, Canada, 1990.
- (12) Edlmann, K.; Hinchliffe, S.; Heinemann, N.; Johnson, G.; Ennis-King, J.; McDermott, C. I. Cyclic CO<sub>2</sub>-H<sub>2</sub>O injection and

residual trapping: Implications for CO<sub>2</sub> injection efficiency and storage security. *Int. J. Greenhouse Gas Control* **2019**, *80*, 1–9.

(13) Peng, X.; Wang, Y.; Diao, Y.; Zhang, L.; Yazid, I. M.; Ren, S. Experimental investigation on the operation parameters of carbon dioxide Huff and puff process in ultra low permeability oil reservoirs. *J. Pet. Sci. Eng.* **2019**, *174*, 903–912.

(14) Yu, W.; Lashgari, H. R.; Wu, K.; Sepehrmoori, K. CO<sub>2</sub> injection for enhanced oil recovery in Bakken tight oil reservoirs. *Fuel* **2015**, *159*, 354–363.

(15) Ma, J.; Wang, X.; Gao, R.; Zeng, F.; Huang, C.; Tontiwachwuthikul, P.; Liang, Z. Study of cyclic CO<sub>2</sub> injection for low-pressure light oil recovery under reservoir conditions. *Fuel* **2016**, *174*, 296–306.

(16) Kong, B.; Wang, S.; Chen, S. In *Simulation and Optimization of CO<sub>2</sub> Huff-and-Puff Processes in Tight Oil Reservoirs*, SPE Improved Oil Recovery Conference, Tulsa, Oklahoma, USA, 2016.

(17) Firouz, A. Q.; Torabi, F. Utilization of carbon dioxide and methane in huff-and-puff injection scheme to improve heavy oil recovery. *Fuel* **2014**, *117*, 966–973.

(18) Wang, X.; Xiao, P.; Yang, Z.; Liu, X.; Wang, L. Laboratory and field-scale parameter optimization of CO<sub>2</sub> huff–n–puff with the staged-fracturing horizontal well in tight oil reservoirs. *J. Pet. Sci. Eng.* **2020**, *186*, No. 106703.

(19) Zhang, Y.; Yu, W.; Li, Z.; Sepehrmoori, K. Simulation study of factors affecting CO<sub>2</sub> Huff and puff process in tight oil reservoirs. *J. Pet. Sci. Eng.* **2018**, *163*, 264–269.

(20) Song, C.; Yang, D. Experimental and numerical evaluation of CO<sub>2</sub> Huff and puff processes in Bakken formation. *Fuel* **2017**, *190*, 145–162.

(21) Cai, Y.; Liu, D.; Pan, Z.; et al. Petrophysical characterization of Chinese coal cores with heat treatment by nuclear magnetic resonance. *Fuel* **2013**, *108*, 292–302.

(22) Xiao, L.; Li, J.; Mao, Z.; et al. A method to determine nuclear magnetic resonance (NMR) T<sub>2</sub> cut off based on normal distribution simulation in tight sandstone reservoirs. *Fuel* **2018**, *225*, 472–482.

(23) Liu, T.; Wang, S.; Fu, R. Analysis of rock pore throat structure with NMR Spectra. *Oil Geophys. Prospect.* **2003**, *38*, 328–333. In Chinese.

(24) Yao, Y.; Liu, D. Comparison of low-field NMR and mercury intrusion porosimetry in characterizing pore size distribution of coals. *Fuel* **2012**, *95*, 152–158.

(25) Li, Z.; Wu, S.; Xia, D.; et al. An investigation into pore structure and petrophysical property in tight sandstones: A case of the Yanchang Formation in the southern Ordos Basin, China. *Mar. Pet. Geol.* **2018**, *97*, 390–406.

(26) Appel, M.; Stallmach, F.; Thomann, H. Irreducible fluid saturation determined by pulsed field gradient NMR. *J. Pet. Sci. Eng.* **1998**, *19*, 45–54.

(27) Lai, J.; Wang, G.; Fan, Z.; Chen, J.; Wang, S.; Zhou, Z.; Fan, X. Insight into the pore structure of tight sandstones using NMR and HPMI measurements. *Energy Fuels* **2016**, *30*, 10200–10214.

(28) Wei, B.; Gao, K.; Song, T.; Zhang, X.; Pu, W.; Xu, X.; Wood, C. Nuclear-Magnetic-Resonance Monitoring of Mass Exchange in a Low-Permeability Matrix/Fracture Model During CO<sub>2</sub> Cyclic Injection: A Mechanistic Study. *SPE J.* **2020**, *25*, 440–450.

(29) Ma, Q.; Yang, S.; Lv, D.; Wang, M.; Chen, J.; Kou, G.; Yang, L. Experimental investigation on the influence factors and oil production distribution in different pore sizes during CO<sub>2</sub> Huff and puff in an ultra-high-pressure tight oil reservoir. *J. Pet. Sci. Eng.* **2019**, *178*, 1155–1163.

(30) Bai, H.; Zhang, Q.; Li, Z.; Li, B.; Zhu, D.; Zhang, L.; Lv, G. Effect of fracture on production characteristics and oil distribution during CO<sub>2</sub> Huff and puff under tight and low-permeability conditions. *Fuel* **2019**, *246*, 117–125.

(31) Singh, H. Impact of four different CO<sub>2</sub> injection schemes on extent of reservoir pressure and saturation. *Adv. Geo-Energy Res.* **2018**, *2*, 305–318.

(32) Li, L.; Su, Y.; Sheng, J. J.; et al. Experimental and Numerical Study on CO<sub>2</sub> Sweep Volume during CO<sub>2</sub> Huff and puff EOR Process in Shale Oil Reservoirs. *Energy Fuels* **2019**, *33*, 4017–4032.